Investigation on nucleation kinetics, crystal growth, structural, optical, dielectric and SHG behaviour of ADP: KDP (85:15) mixed crystal grown using seed rotation method for nonlinear optical applications

G. IYAPPAN*, P. RAJESH, P. RAMASAMY
Department of Physics, SSN College of Engineering, Kalavakkam, Tamil Nadu, India

Mixed crystal of ammonium dihydrogen phosphate (ADP) and potassium dihydrogen phosphate (KDP) has been grown using aqueous solution method by temperature lowering seed rotation technique. The grown mixed crystal has a positive temperature coefficient of solubility. Metastable zone width and induction period have been determined and analysed. The lattice parameters of the grown mixed crystal have been obtained by single-crystal X-ray diffraction analysis. The optical transmission spectrum of the mixed crystal was recorded using UV-Vis-NIR spectrum. Second-harmonic generation (SHG) studies were carried for the pure ADP, KDP and ADP: KDP (85:15) mixed crystals. It was found that the SHG efficiency of the mixed crystal is 1.5 times that of pure KDP. The dielectric measurements were used to analyse the dielectric constant and dielectric loss of the mixed crystal.

(Received July 8, 2019; accepted June 16, 2020)

Keywords: Mixed crystals, Nucleation, Solubility, Solution growth

1. Introduction

The ammonium dihydrogen phosphate, $NH_4H_2PO_4$ (ADP) crystal has gained importance due to their dielectric, antiferroelectric and nonlinear optical properties finding applications in electro-optical modulators, harmonic generators and as monochromators for X-ray fluorescence analysis [1-4]. The potassium dihydrogen phosphate, KH_2PO_4 (KDP) crystal exhibits excellent electro-optical and nonlinear optical properties and is commonly used in frequency conversion applications such as second, third and fourth harmonic generation and in electro-optical modulation [3-5]. Such excellent applications of ADP and KDP crystals encourage researchers to grow large plates of these crystals for the fabrication of electro-optic switches and frequency converters [6-7]. During the last three decades many significant results are published by various researchers on pure ADP and KDP crystals [8-10]. Though the researchers are focussing on the growth of ADP and KDP crystals, it is evident from the literature that mixing of these crystals in selected concentration would lead the enormous enhancement of the various properties which are very useful to overcome the existing complications in the preparation of SHG elements [11-13]. A mixed crystal has physical properties analogous to those of pure crystals. The composition dependence varies from system to system and property to property [14]. In many cases, the property changes monotonically with composition in a linear or nearly linear manner. Once the trend in composition dependence is established, we have a means to have a tailor-made crystal with a desired value for a given physical property, e.g optical, electrical, thermal and mechanical [13,15-16]. The mixed crystals of ADP and KDP attract much attention because of the interesting spin-glass state in a certain intermediate mixing concentration range due to the competing antiferroelectric and ferroelectric interaction [17]. Xiue Ren et. al., have investigated the fundamental growth process of ADP and KDP experimentally and theoretically [18]. Srinivasan et. al., have investigated the different molar ratio concentrations of the mixed crystals [14]. There already exist some preliminary investigations on mixed crystals grown by conventional technique [7, 19-20]. But none of them is complete in the sense of studying the concentration dependence of physical properties of ADP: KDP mixed crystal with wide variations in the concentration. In this point of view, the present study aims to enhance the existing properties of ADP by mixing KDP in an appropriate ratio. The fundamental parameters such as interfacial tension (γ), induction period (τ), critical radius(r^*), number of molecules in the critical nucleus (i*), and Gibb's free energy (ΔG^*) have been optimized in order to grow large size crystals [21-23]. Growth of ADP: KDP mixed crystals in certain concentration is identified as difficult to grow in large size because of their large mismatch in lattice constants between KDP and ADP (lattice constants of ADP: a^A=0.7530 nm, c^A=0.7542 nm; lattice constants of KDP: a^K=0.7430 nm, c^K=0.697 nm) [24]. In the present work, it is proposed to study the nucleation kinetics parameters and to grow bulk size

mixed crystals of ADP and KDP, in the ratio of 85:15. The observed results are analysed and discussed in detail.

2. Experimental

2.1. Solubility studies

The size and growth rate of a crystal depends on the solubility and temperature of the solution. According to thermodynamics, when the chemical potential of the pure solute in the saturated solution is equal to the chemical potential of the same solid then it is called as solubility and it depends on the temperature and pressure. Pure ADP and KDP have been purified several times by recrystallization using deionized water as a solvent. The purified ADP and KDP materials with 85:15 ratio have been taken and dissolved completely in deionized water. The resistivity of the used deionized water is 18.2 MΩ cm. The recrystallized mixed materials were used for the solubility study. The solubility data of pure ADP and KDP is available in the literature and it is used for the present work. The solubility of ADP: KDP (85:15) in deionized water was assessed as a function of temperature, in the range from 30 ºC to 50 ºC in steps of 5 ºC. The saturated solution was allowed to reach the equilibrium at a chosen temperature and then the solubility was gravimetrically analysed. Studies were carried out in a constant temperature water bath (CTB) with a cryostat facility with an accuracy of ±0.01ºC. Comparing the results with the pure ADP, it is found that the mixing of KDP has decreased the solubility of the pure ADP. The solubility curve is shown in Fig. 1.

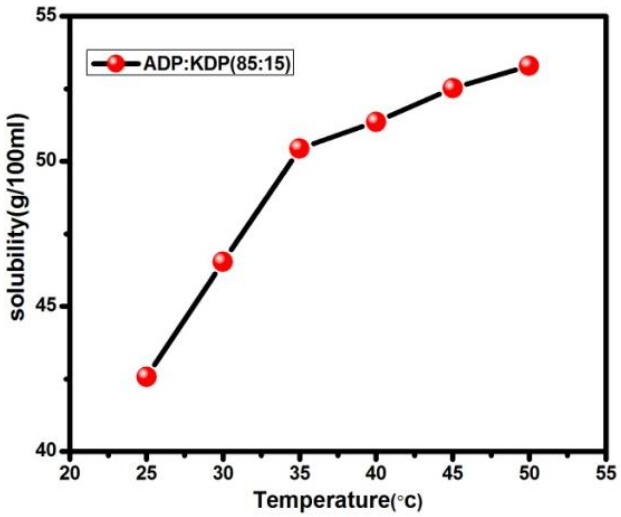

Fig. 1. Solubility curve of ADP: KDP (85:15) mixed crystal

2.2. Determination of metastable zone width

Metastable zone width is an important process for crystal growth that carefully controls the number of nuclei and crystallites under the conditions where the super-saturation varies in time [25-26]. The stability of the growth solution with wide metastable zone width is also important for the growth of large crystals. The meta-stable zone width studies of ADP: KDP (85:15) were carried out by adopting the polythermal method [27-28]. The ADP: KDP (85:15) saturated solution was prepared at 25 ºC according to solubility diagram, then the solution was overheated to 5 ºC above its saturation temperature to get higher homogeneity. Further, it was slowly cooled at a desired cooling rate of 5 ºC per hour until the first nucleation seen. At 21.8 ºC a visible speck was observed which represents the nucleation temperature. The difference between saturation and nucleation temperature is the metastable zone width of the solution. The experiment was repeated for various temperatures (30ºC, 35ºC, 40ºC, 45ºC, 50ºC) and corresponding metastable zone widths were measured. Fig. 2 shows the metastable zone width of the mixed ADP: KDP (85:15).

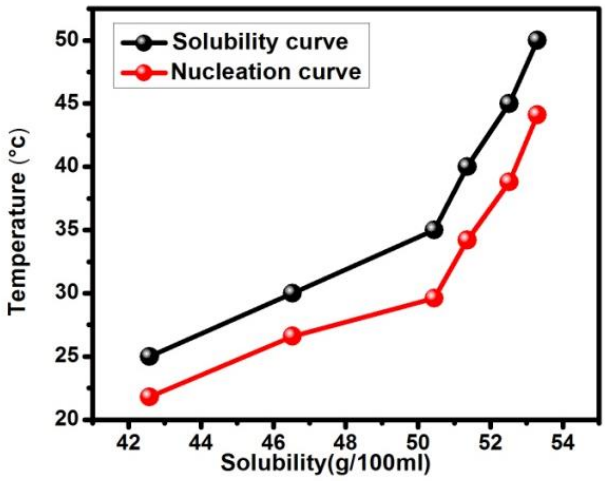

Fig. 2. Solubility and metastable zone width of ADP: KDP (85:15) mixed crystal (color online)

2.3. Induction period measurements

Induction period experiment was performed at selected degrees of supersaturation (S), viz, 1.05, 1.06, 1.07, 1.08 and 1.09 at 40 ºC by an isothermal method. The supersaturated solution was prepared and the required level of supersaturation was achieved by dissolving the required amount of ADP: KDP (85:15) in deionized water. The first speck was seen at the bottom of the container and the same procedure has been repeated for different supersaturation ratios. The observed values are plotted and shown in Fig. 3.

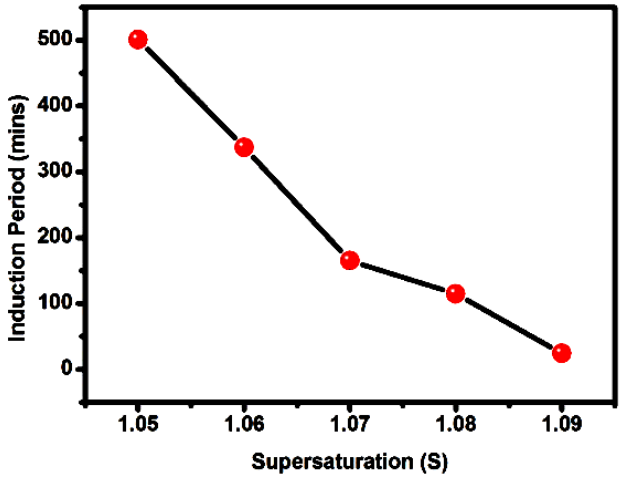

Fig. 3. Induction period vs Supersaturation ratio

The interfacial tension has been calculated using induction period values [29].

$$\ln \tau = \ln \mathrm{B} + \left(\frac{16\pi\gamma^3}{3R^3T^3(\ln S)^2} \right) \quad (1)$$

where, R is the gas constant, N_A is the Avogadro's number & $ln\ B$ depends on temperature.
where,

$$\gamma^3 = \frac{3R^3T^3m}{16\pi V^2 N_A^3} \quad (2)$$

The plot of ln τ against 1/ (ln S) 2 is shown in Fig. 4. The number of molecules in the critical nucleus is expressed by

$$i^* = \frac{4\pi(r^*)^3}{3v} \quad (3)$$

The free energy required to form a spherical nucleus is given by

$$\Delta G = \frac{4}{3}\pi r^3 \Delta G_v + \pi 4r^2\gamma \quad (4)$$

where, ΔG_V is the energy change per unit volume and r is the radius of the nucleus. At the critical state, the free energy of formation obeys the condition d (ΔG)/dr = 0. Hence the radius of the critical nucleus is expressed as [22]

$$r^* = -2/\Delta G_v \quad (5)$$

The radius of the critical nucleus as a function of supersaturation is shown in Fig. 5. Using the classical theory of nucleation the volume excess free energy is written as

$$\Delta G_v = -\Delta\mu/V \quad (6)$$

where,

$$\Delta_\mu = kT \ln S \quad (7)$$

where, V is the molecular volume, T is the particular saturation temperature, S is supersaturation ratio and k is the Boltzmann constant. The critical free energy is given by [23]

$$\Delta G^* = 16\gamma^3/3(\Delta G_v)^2 \quad (8)$$

Based on the experimental data i.e., using the interfacial tension values, interfacial energy values, Gibbs free energy per unit volume (ΔG_v), critical free energy (ΔG^*), have been calculated. The values are given in table 1. As the supersaturation increased, the radius of critical nucleus decreased, and critical radii were evaluated and it was found that it is decreased from 7.7 nm to 4.2 nm for ADP: KDP (85:15) for the supersaturation range from1.05 to1.09. At 40 ºC, lowest supersaturation point S=1.05 produced no nucleation up to 30,060 seconds, whereas the supersaturation point S=1.09 farmed nucleation even at 1,440 seconds. It is observed from these results, the induction period decreases with increase in supersaturation as expected from the classical nucleation theory.

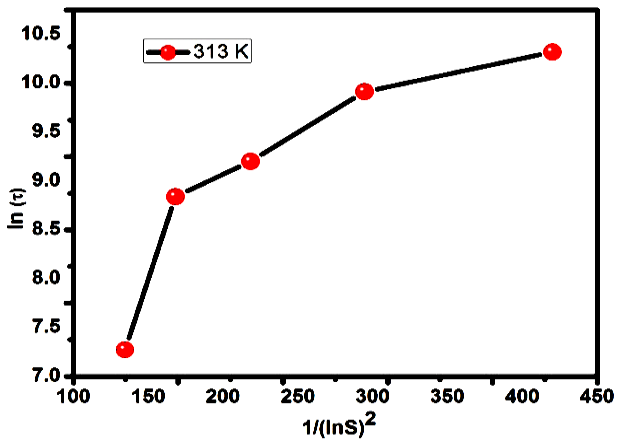

Fig. 4. ln (τ) vs $(lnS)^{-2}$ of ADP: KDP (85:15)

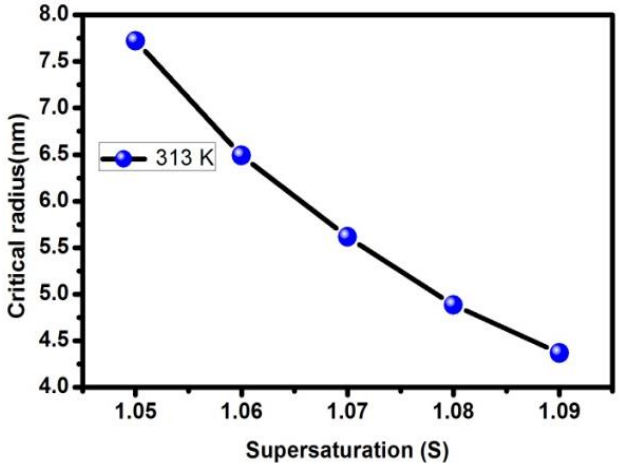

Fig. 5. Critical radius as a function of supersaturation

Table 1. Nucleation Kinetics parameter of ADP: KDP (85:15) *mixed crystal at 313 K*

S	τ (s)	$\Delta G_v \times 10^6$ J/m^2	$\Delta G_v \times 10^{-19}$	r* (nm)	i^*
1.05	30,060	-0.496	1.435	7.721	4547.00
1.06	20,220	-0.590	1.014	6.491	2701.55
1.07	9,900	-0.682	0.759	5.615	1748.87
1.08	6,900	-0.784	0.574	4.885	1151.60
1.09	1,440	-0.877	0.459	4.367	822.00

2.4. Crystal growth

KDP (85:15) mixed crystals were grown from aqueous solution by accelerated crucible rotation technique (ACRT). The crystals were grown using an apparatus which can control the forced convection configurations to maintain homogeneity of the solution. This apparatus consists of a seed rotation controller coupled with a stepper motor, which is controlled by using a microcontroller-based drive. This controller rotates the seed holder in the crystallizer in forward and backward directions. The uniform rotation of the seed is required so as not to produce stagnant regions or recirculating flows, otherwise inclusions in the crystals will be formed due to inhomogeneous supersaturation in the solution. The applied rotations and cycles were 40 rpm and 20 on both sides, respectively. The crystal growth was carried out in a 5000 ml standard crystallizer used for conventional crystal growth method of slow cooling along with the seed rotation. 3000 ml saturation solution of ADP: KDP (85:15) was prepared and the saturation temperature was 45 ºC. The solution was filtered by Whatman filter paper of pore size 11 µm. After the filtration, the temperature of the solution was increased to 55 ºC for about 12 hours. Then the temperature has been reduced to saturation temperature of 45 ºC in steps of 1 ºC per hour. In the centre of the crystallizer 5x5x5 mm^3 size ADP crystal was fixed and it was kept inside a constant temperature bath. The crystallizer temperature fluctuation is less than 0.01 ºC. From the saturation point (45 ºC), the temperature was decreased at the rate of 0.02 ºC per hour. Since the seed crystal size was 5×5×5 mm^3 in the initial stage itself 40 rpm was given on both the growth period. After 20 days of growth good quality crystals were harvested. The size of the grown crystal is 45×10×10 mm^3. The grown ADP: KDP (85:15) crystal is shown in Fig. 6.

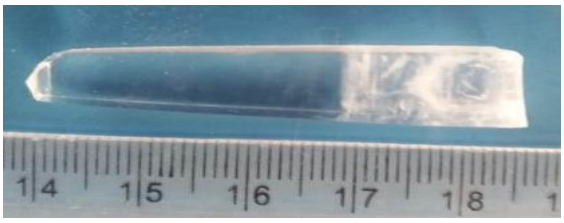

Fig. 6. ADP: KDP (85:15) mixed crystal

3. Characterization

The grown mixed crystals were subjected to different characterization techniques. The lattice parameters of the grown mixed crystals have been studied by single crystal X-ray diffraction analysis with MoKα radiation. Powder X-Ray diffraction analyses for the grown mixed crystals ADP: KDP (85:15) were determined with using X'Pert PRO X-ray diffractometer analytical, Netherland using CuKα radiation in the 2θ range of 15-80 to determine the phase of the crystals. The linear optical property of crystals was carried out using PerkinElmer Lambda-35 UV-Vis-NIR spectrometer in the range of 200-1100 nm. To analyze the second harmonic generator properties, the Kurtz and Perry powder SHG test was performed on the grown mixed crystals using a Q-switched Nd:YAG laser. The dielectric measurements were carried out and dielectric constant and dielectric loss calculated using the relation $\varepsilon_r = C_{crys}/C_{air}$. Where C_{crys} is the capacitance of the crystal and C_{air} is the capacitance of same dimension of air. The dimension of the sample is 5 × 5 × 2 mm^3 and coated on both faces using silver paste to form a parallel plate capacitor between the two copper electrodes.

4. Results and discussion

4.1. XRD analysis

The X-ray diffraction pattern of the crystal was recorded using a Philips model pw 1710 with nickel-filtered Mokα radiations (35 kV, 10 mA) of wavelength 1.5418 Å. It is observed from single crystal XRD studies that the grown mixed crystal ADP: KDP (85:15) belong to tetragonal system and corresponding lattice parameters are a= 7.53 Å, b=7.53 Å, c= 7.48 Å, α=90, β=90, γ=90. The volume of the unit cell is 424 Å^3. Both the ADP and KDP crystals are belonging to the same system and it is understood from the results that the addition of 15% of

KDP in ADP has not distorted the internal structure of the ADP. The powder XRD analysis has been used to confirm the crystalline phase of the mixed crystals. The mixed crystal has been ground nicely and subjected to the XRD analysis. The samples were scanned in steps of 0.05° between the 2θ angle ranges 15° to 50°. The observed prominent phases of the grown mixed ADP: KDP (85:15) crystals are (101), (200), (211), (220), (301), (312), it is similar to the ADP crystals but the intensities are found to be varied. This may be due to the presence of KDP in the lattice of ADP. The recorded powder XRD pattern is shown in the Fig. 7. It is in good agreement with the reported results [30].

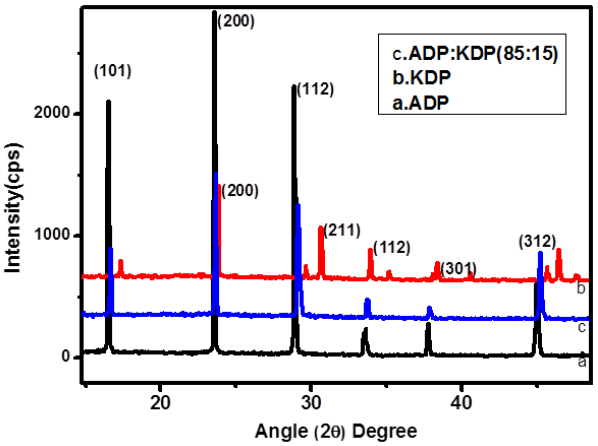

Fig. 7. Powder XRD pattern of the mixed crystals (color online)

4.2. UV-Vis NIR optical studies

Crystal plates of cut and polished mixed crystal with a thickness of 2 mm without any antireflection coating were used for optical measurements. The optical transmission of the sample was recorded in the wavelength range of 200-1100 nm. Mixed crystals show good transmission in the entire visible region and confirm the quality of the grown mixed crystals. It is known from the literature that ADP: KDP with 90:10 ratio has 80% of transparency [7]. In the present case, almost similar transparency has been recorded. In order to confirm the reproducibility, several times the beam was passed through the various regions of the crystals and the same results were observed. The spectrum is shown in the Fig. 8. It is observed from the figure that the presence of KDP molecules in the lattice sites of ADP has not affected the optical transparency. This clearly shows the ADP crystal lattice can accommodate the KDP molecules up to certain extent. Good transparency in entire visible region confirms the suitability for the fabrication of optical devices. The cut off wavelength was below 200 nm. The absorption coefficient was calculated from the transmission spectrum using the below equation [31-32].

$$\alpha = \frac{2.3026}{t}\log_{10}\left(\frac{100}{T}\right) \qquad (9)$$

where T is the Transmittance in % and t is the thickness of the grown mixed crystal. The direct band gap energy was calculated by using the below formula,

$$\alpha h\nu = \mathrm{A}\left(h\nu - \mathrm{E}_g\right)^{\frac{1}{2}} \qquad (10)$$

where, E_g is the optical band gap of the crystal, A is the constant, v is the frequency of the incident light [33]. The direct optical band gap of grown mixed crystal was calculated by the plotting $(\alpha h\nu)^2$ versus $(h\nu)$. Fig. 9 shows the band gap value of grown mixed crystals. The direct optical band gap of mixed crystal is found to be 4.5 eV. Large band gap of the grown crystal implies that this can be used for the NLO applications [34].

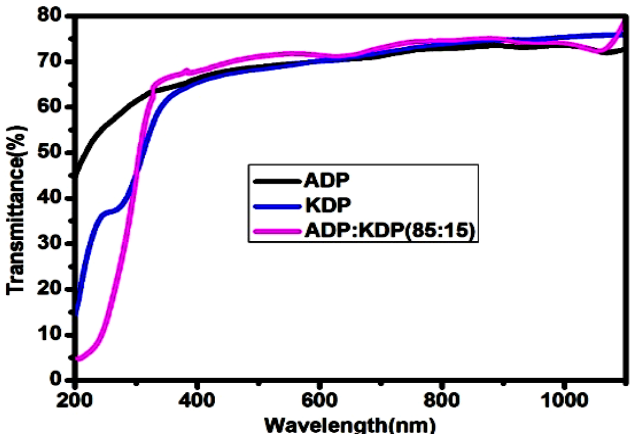

Fig. 8. UV-Vis-NIR spectra of grown mixed crystal (color online)

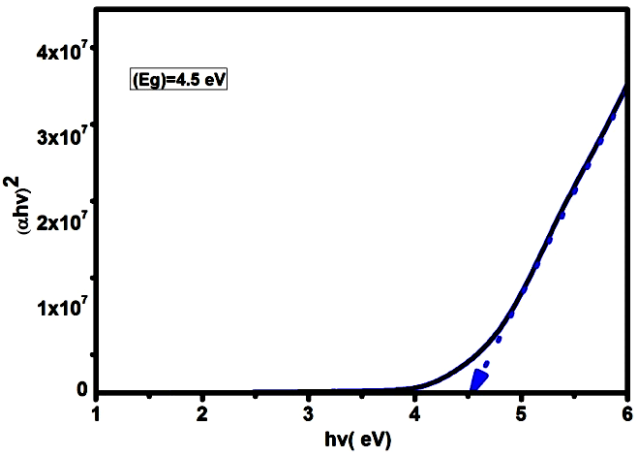

Fig. 9. Bandgap energy graph of grown mixed crystal

4.3. SHG efficiency analysis

In order to measure the SHG efficiency, the grown mixed crystals were powdered and subjected to Kurtz and Perry powder technique. Fig. 10 shows the detailed experimental setup of Kurts and Perry powder technique. The conversion efficiency of mixed crystal was found

using the Q-switched mode Nd:YAG laser operating at 1064 nm with the repetition rate of 10 Hz and pulse with 8 ns. The emission of sharp green light as the output confirms the SHG behaviour of mixed crystals. No degradation of material during or in mid-term of the SHG measurement was observed. The observed values of grown crystal and the reference materials are given in table 2 in mV. The values clearly indicate that the grown mixed crystal has slightly increased compared to ADP and it is 1.5 times compared to the pure KDP. The improvement of SHG effect is based on the enhancement of orbital hybridization or reduction of charge transfer energy, which results in the widened bandwidth of occupied state [11]. In this case the larger the bandwidth of the mixed crystal leads to the improvement in the SHG efficiency. Higher SHG efficiency of mixed crystal indicates the suitability of the crystal for harmonic generation applications.

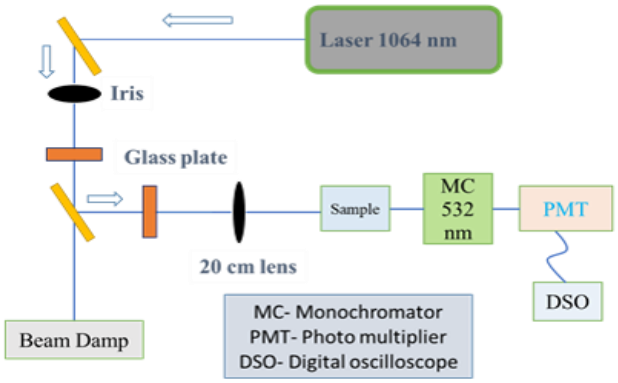

Fig. 10. Powder SHG experimental setup (color online)

Table 2. SHG efficiency of grown ADP: KDP (85:15) *mixed crystal*

S.no	Crystal	SHG efficiency
1	Pure ADP	30mV
2	Pure KDP	24mV
3	ADP : KDP (85:15)	34mV

4.4. Dielectric measurements

A study on the dielectric properties of crystals gives an electric field distribution within crystal. The frequency and temperature dependence of dielectric properties gives great insight into the materials applications. The dielectric constant and dielectric loss have been carried out using conventional parallel plate capacitor method with Agilent 428 LCR meter at various temperatures and various frequencies with the range of 1 kHz, 10 kHz, and 100 kHz, and 1 MHz. As grown high quality mixed crystals both side coated with silver paste have been used for the measurements. The dielectric constant of the mixed crystal has been calculated using the following formula [35-36].

$$\varepsilon_r = C_{crys}/C_{air} \quad (11)$$

where C_{crys} is the capacitance of the crystal and C_{air} is the capacitance of the same dimension of air. Fig. 11(a) and 11(b) shows dielectric constant and dielectric loss of the mixed crystal. Several results have been already reported by various researchers about the dielectric nature and phenomena of the ADP and KDP [37, 38]. It is observed from the figure that the frequency increases with decrease in the dielectric constant and similarly when temperature increases dielectric constant is increased. The large value of dielectric constant at low frequency is may be due to the presence of all the four polarizations, namely space charge, orientation, electronic and ionic polarization. The decrease in dielectric constants at higher frequencies is attributed to the significant decrease in these polarizations and absence of space charge polarization near the grain boundary interface [39]. The low dielectric loss at high frequency implies that the optical quality of the crystal is higher because of lesser defects, which is a desirable property for NLO applications. Also the dielectric constant of ADP: KDP (85:15) are higher than the pure ADP and KDP [7]. These results indicate that the grown mixed crystals of ADP: KDP (85:15) has dielectric nature and suitable for the NLO applications.

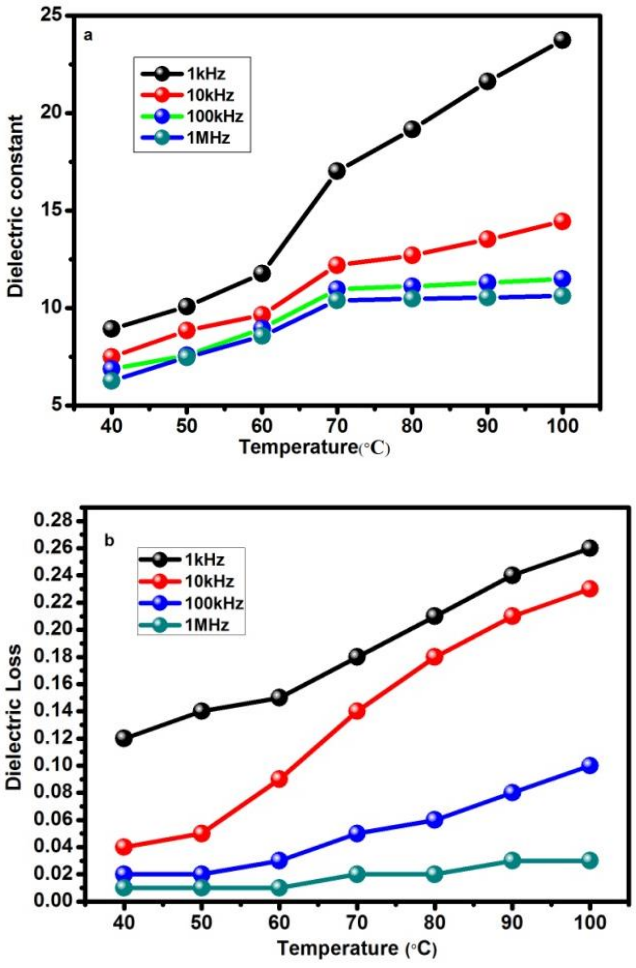

Fig. 11. (a) The temperature dependence of dielectric constant, (b) The dielectric loss of the grown mixed crystal (color online)

5. Conclusion

The solubility study indicates that mixing of 15% of KDP decreasing the solubility of ADP. The metastable zone width and induction periods were determined systematically. The nucleation kinetics of ADP: KDP (85:15) were studied and the optimized induction period was determined in order to control nucleation rate and to grow a good quality crystal. Mixed crystals of ADP: KDP (85:15) have been grown successfully by the temperature lowering seed rotation technique. The transmission spectrum of the mixed crystal reveals that the grown crystal has 70% transparency in the entire visible region. From the Kurtz and Perry powder technique, it is found that SHG efficiency is 1.5 times that of pure KDP crystal. It is concluded that the high SHG efficiency, wide bandwidth, high transmittance and low dielectric loss of the grown ADP: KDP (85:15) mixed crystal indicate the suitability of the crystals for the preparation of SHG elements.

Acknowledgements

The authors gratefully acknowledge Council of Scientific and Industrial Research (CSIR), Government of India for the financial support [Ref: no. 03 (1362/16/EMR-II].

References

[1] G. Bhagavannarayana, S. Parthiban, Meenakshisundaram, Crystal Growth and Design **8**, 446 (2007).
[2] G. Ramasamy, S. Meenakshisundaram, Journal of Crystal Growth **352**, 63 (2012).
[3] M. Shanmugham, F. D. Gnanam, P. Ramasamy, Journal of Materials Science Letters **5**, 174 (1986).
[4] P. Shenoy, K. V. Bangera, G. K. Shivakumar, Materials Science and Engineering **167**, 206 (2010).
[5] P. Rajesh, P. Ramasamy, Optical Materials **42**, 87 (2015).
[6] SahilGoel, Nidhi Sinha, Harsh Yadav, Abhilash, J. Joseph, Abid Hussain, Binay Kumar, Arabian Journal of Chemistry **13,** 146 (2020).
[7] P. Rajesh, P. Ramasamy, G. Bhagavannarayana, Journal of Crystal Growth **362**, 338 (2013).
[8] N. Zaitseva, L. Carman, Progress in Crystal Growth and Characterization of Materials **43,** 1 (2001).
[9] J. Lasave, S. Koval, N. S. Dalal, R. L. Migoni, Physical Review Letters **98**, 267601 (2007).
[10] Youping, Zeng Jinbo, Wu Dexang, Su Genbo, Yan Mingshan, Journal of Crystal Growth **169**, 196 (1996).
[11] Zhi Li, Qiong Liu, Ying Wang, Toshiaki Iitaka, Haibin Su, Takami Tohyama, Zhihua Yang, Shilie Pan, Physical Review B **96**, 035205 (2017).
[12] Jibin Wen, Feng Geng, Fengrui Wang, Jin Huang, Xiaodong Jiang, Qinghua Deng, Linhong Cao, Crystal Research and technology 1800010 (2018).
[13] G. Iyappan, P. Rajesh, P. Ramasamy, Optoelectron. Adv. Mat. **13**, 217 (2019).
[14] K. Srinivasan, P. Ramasamy, A. Cantoni, G. Bocelli, Materials Science and Engineering **B52**, 129 (1998).
[15] J. J. Kim, W. F. Sherman, Physical Review B **36**, 5651 (1987).
[16] Duanliang Wang, Tingbin Li, Shenglai Wang, Jiyang Wang, Chuanying Shen, Jianxu Ding, Weidong Li, Pingping Huang, Chengwei Lu, Optical Materials Express **7**, 533 (2017).
[17] B. K. Choi, J. J. Kim, Physical Review B **28**, 1623 (1983).
[18] Xiue Ren, Dongli Xu, Dongfeng Xue, Journal of Crystal Growth **310,** 2005 (2008).
[19] S. Sen Gupta, T. Kar, S. P. Sen Gupta, Materials Chemistry and Physics **58**, 227 (1999).
[20] Lisong Zhang, Fang Zhang, Mingxia Xu, Zhengping Wang, Xun Sun, RSC Adv. **5**, 74858 (2015).
[21] S. Chandran, R. Paulraj, P. Ramasamy, Journal of Crystal Growth **468,** 68 (2017).
[22] A. Silambarasan, P. Rajesh, P. Ramasamy, Journal of Crystal Growth **409,** 95 (2015).
[23] P. V. Dhanaraj, N. P. Rajesh, C. K. Mahadevan, G. Bhagavannarayana, Physica B: Condensed Matter **404**, 2503 (2009).
[24] Z. De-Gao, T. Bing, W. Shu-Hua, J. Xue-Jun, L. Ming, L. H. Lin-Xiang, H. Wan-Xia, Crystal Research and Technology **44**, 925 (2009).
[25] K. Sangwal, Crystal Growth and Characterization of Materials **36**, 163 (1998).
[26] K. Sangwal, Crystal Growth and Characterization of Materials **32**, 3 (1996).
[27] K. Sangwal, Mielniczek-Brzoska, E, Barylska, S, Chemical Engineering Research and Design, **92**, 491 (2014).
[28] Keshra Sangwal, Ewa Mielniczek-Brzóska, Jarosław Borc, Crystal Research and Technology **48**, 956 (2013).
[29] G. H. Sun, G. H. Zhang, X. Q. Wang, Z. H Sun, D. Xu, Chemistry and Physics **122,** 524 (2010).
[30] Dongli Xu, Dongfeng Xue, Journal of Crystal Growth **286**, 108 (2006).
[31] R. N. Shaikh, M. D. Shirsat, P. M. Koinkar, S. S. Hussaini, Optics & Laser Technology **69**, 8 (2015).
[32] P. Karuppasamy, M. S. Pandian, P. Ramasamy, Journal of Crystal Growth **473**, 39 (2017).
[33] P. Rajesh, P. Ramasamy, G. Bhagavannarayana, Journal of Crystal Growth **311**, 4069 (2009).
[34] D. Kalaiselvi, R. Jayavel, Applied Physics A **107**, 93 (2012).
[35] K. Thukral, N. Vijayan, D. Haranath, K. K Maurya, J. Philip, V. Jayaramakrishnan, Arabian Journal of Chemistry **12**, 3193 (2019).
[36] K. Boopathi, P. Rajesh, P. Ramasamy, P. Manyum, Optical Materials **35**, 954 (2013).
[37] M. Anis, S. S. Hussaini, M. D Shirsat, R. N Shaikh, G. G Muley, Materials Research Express **3**, 106204 (2016).
[38] P. Rajesh, A. Silambarasan, P. Ramasamy, Materials Research Bulletin **49**, 640 (2014).
[39] Mahendra Shirsat, Mohd Anis, A. B. Gambhire, Hussaini Shuakat, Materials Research Express **1,** 015016 (2014).

*Corresponding author: iyappanyuva1992@gmail.com